

Effect of Post Annealing on Structural and Optical Propertie of SnO₂ Thin Films Deposited By Dc Magnetron Sputtering

Salah Kaduri Haza'a

Physics Department , Education College, Al-Mustansiriyah University, Baghdad. Iraq.

Abstract: SnO₂ thin films were deposited on glass at 200°C substrates temperature by DC magnetron sputtering technique. The prepared films were annealed in air at temperatures of 300 °C, 400 °C and 500 °C for 1 h. The effects of annealing on the structural and optical properties of the films were investigated by X-ray diffractometer and UV/VIS spectrophotometer. X-ray diffraction patterns indicated that the SnO₂ films had a polycrystalline tetragonal structure. The crystallinity levels of the films from the structural parameters such as diffraction angle, lattice parameters, unit cell, grain size, dislocation density and texture coefficient were calculated and analyzed. Optical transmission is found to increase with annealing. Band gap energy, Urbach energy and optical constants were also investigated. Also, the dispersion parameters such as single oscillator energy and dispersive energy have been discussed in terms of the Wemple-DiDomenico single-oscillator model.

Keywords: SnO₂, DC. magnetron sputtering, Annealing, Structure, Optical transmittance, Dispersion parameters

I. Introduction

Transparent conducting oxide (TCO) thin films are of great interest due to its variety of applications. Consequently, thin films with high electrical conductivity and optical transparency have been a subject of investigation since last century. SnO₂ belongs to the important class of transparent conductor oxide materials that combine low electrical resistance with high optical transparency in the visible range of the electromagnetic spectrum. These properties are required for optoelectronic applications i.g light emitting diodes, electrode materials in solar cells, flat panel displays, transparent field effect transistors [1,2].

SnO₂ thin film has been prepared by various techniques such as magnetron sputtering [3,4], electron beam evaporation [5], sol gel coating [6], chemical vapor deposition [7], etc. Among them DC reactive magnetron sputtering is one of the most useful technique having high deposition rates, uniformity over large areas of the substrates and easy control over the composition of the deposited films. In this work, SnO₂ thin films have been deposited by sputtering at 200 °C temperature and subsequently annealed in air at different temperature. Then, they have been analyzed comparatively by structural and optical measurements. The objective is to get a better understanding of the relationships between the different characteristics of the SnO₂ thin films and a detailed investigation of the effect of annealing on structural and optical properties of SnO₂ thin films.

Experimental: The SnO₂ films were prepared by DC magnetron sputtering on glass substrate at temperature 200°C. The vacuum was evacuated by an Edwards 306 pumping system, the vacuum chamber was exhausted by an oil-diffusion pump at 2×10^{-6} Torr in around 30 minutes, in an atmosphere of argon and oxygen Ar 95% and O₂ 5% respectively, DC power 50W and magnetic field 370 gauss and the distance between the cathode and the substrate holder was 30 mm. Tin Oxide was sputtered from targets on the glass substrate. The targets material are in the form of plates with 60mm diameter and 2mm thickness and made from SnO₂ powder. After deposition process, films were annealed in air ambient at different temperatures of 300, 400 and 500 °C for 1 h. The crystal structure and optical properties of the films were analyzed by using x-ray diffraction (XRD) and UV/VIS/NIR spectrophotometer with a double beam in the wavelength range of (300-900) nm. The film thickness was measured by Scanning Electron Microscope (SEM). The film thickness was measured to be about (800±10 nm) using the cross-section scanning electron microscopy (SEM) image as shown in Fig(1).

II. Results And Discussion

Fig(2) shows the XRD spectra of SnO₂ thin films as-deposited at 200 °C and annealed in air for 1 h at different temperatures (300, 400 and 500 °C). From these spectra, it was seen that all films have a polycrystalline structure of tetragonal form SnO₂, which were confirmed from the SnO₂ JCPDS card [8]. Diffraction peaks belonging to (110) (101) and (200) planes were observed in all the SnO₂ thin films, and some low intensity peaks corresponding to the orientations (211), (220) and (002). Further, no other impurity peak was observed in the XRD pattern showing the single phase sample formation. As can also be seen from Table 1, slightly deviations in the diffraction angles of the crystal planes before and after annealing. This may be due to the formation of different strain relief at the crystal grains [9].

In order to investigate variation of lattice parameters of the SnO₂ films with thermal annealing temperature, lattice constant 'a' and 'c' and the volume of the unit cell 'V' for the tetragonal phase structure is determined by the relations[10]:

$$1/d^2 = (h^2 + k^2)/ a^2 + l^2/c^2 \quad \dots\dots\dots(1)$$

$$V = a^2c \quad \dots\dots\dots(2)$$

Where (hkl) is miller indices. It is concluded that these values given in Table 2, almost agree with those obtained from the JCPDS card for polycrystalline SnO₂ powder of tetragonal structure [8]. As seen from Table 2, the volume of the unit cell value of the SnO₂ films slightly increases with the annealing temperature. The grain size (crystalline sizes) 'D' values before and after annealing process of about 14.4 nm and 26.3 nm as in Table 3 obtained from the well known Scherrer equation [10]:

$$D = k' \lambda / \beta \cos\theta \quad \dots\dots\dots(3)$$

Where 'k'' varies from 0.89 to 1.39. But in most of the cases it is closer to 0.9. Hence for grain size calculation it is taken as 0.9, 'λ' is wavelength of X-ray, 'β' is the full-width at half of the peak maximum in radians and 'θ' is Bragg's angle.

Additionally, the dislocation density 'δ' listed in Table 3 and defined as the length of dislocation lines per unit volume of the crystal, was calculated by the relation [6] :

$$\delta = 1/(D)^2 \quad \dots\dots\dots(4)$$

The crystallization levels of the films annealed at 300°C is best because of their low δ values which represent the amount of defects in the film. Larger 'D' and smaller 'δ' values indicate better crystallization of the material. The texture coefficient 'T_C' for the (hkl) orientations were estimated from the following relation [11,12]:

$$T_C = \frac{I_{(hkl)}}{I_{(hkl)}^0} \frac{1}{\sum_n \frac{I_{(hkl)}}{I_{(hkl)}^0}} \quad \dots\dots\dots(5)$$

Where 'I_(hkl)' is the measured intensities, 'I_(hkl)⁰' corresponding to recorded intensities according to the JCPDS. 'N' is the reflection number and n is the number of diffraction peaks. A sample with randomly oriented crystallite yields T_{C(hkl)} = 1, while the larger this value, the larger abundance of crystallites oriented at the (hkl) direction. The calculated texture coefficients T_C are presented in Table 3. It can be seen that the highest 'T_C' is obtained for the (200) plane of the SnO₂ thin film annealed at 300 °C. The higher values of texture coefficient reveal that the tin oxide film crystallinity is improved after thermal annealing[11,12].

Table .1. Interplanar spacing of various planes for the SnO₂ thin films.

Samples	Standard values		As- deposited at 200°C			Annealed at 300°C			Annealed at 400°C			Annealed at 500°C		
	(hkl)	2θ	d(Å)	2θ	d(Å)	d%	2θ	d(Å)	d%	2θ	d(Å)	d%	2θ	d(Å)
(110)	26.61	3.351	26.58	3.350	0.03	26.81	3.323	0.80	26.67	3.339	0.34	26.69	3.336	0.44
(101)	33.89	2.644	33.88	2.643	0.04	34.09	2.628	0.60	33.97	2.637	0.26	33.99	2.635	0.34
(200)	37.95	2.369	37.89	2.373	0.12	38.14	2.358	0.46	37.99	2.366	0.13	38.02	2.365	0.17

Table .2. Lattice constant values of SnO₂ thin films.

Lattice Parameter	Standard values	As-deposited at 200°C	Annealed at 300°C	Annealed at 400°C	Annealed at 500°C
a (Å)	4.738	4.739	4.567	4.723	4.757
c (Å)	3.188	3.315	3.212	3.178	3.164
V (Å) ³	71.60	74.48	66.99	70.90	71.62

Table .3. Variation of grain size , dislocation density and texture coefficient of SnO₂ thin films with annealing temperature.

Samples	Grain size nm D (hkl)			Dislocation density 10 ¹⁴ m ⁻² δ (hkl)			Texture coefficient T _C (hkl)		
	(110)	(101)	(200)	(110)	(101)	(200)	(110)	(101)	(200)
	As- deposited at 200°C	24.6	16.2	22.2	16.5	38.1	20.3	0.86	0.755
Annealed at 300°C	26.3	17.9	22.3	14.4	31.2	21.9	0.92	0.73	1.44
Annealed at 400°C	22.3	15.8	20.3	20.6	40.1	24.3	0.77	0.76	1.48
Annealed at 500°C	23.3	15.4	18.7	18.4	42.2	28.5	0.9	0.73	1.37

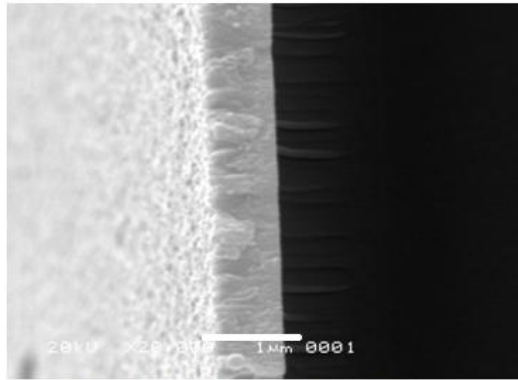


Fig.1. SEM picture of SnO₂ thickness

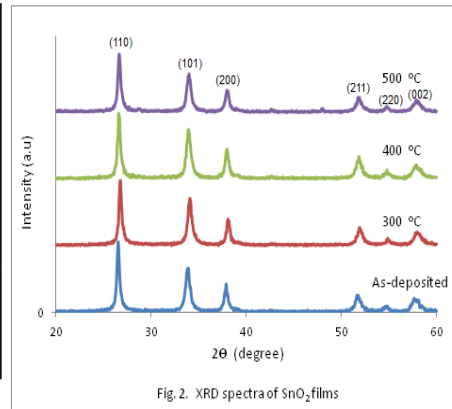


Fig.2. XRD spectra of SnO₂ films

The optical transmittance spectra of all films are presented in Fig(3). The average optical transmittance in the wavelength region (from 500 to 900 nm) of SnO₂ thin films before thermal annealing is 77.5%, while after annealed at 300°C, 400°C and 500°C, the transmittance is 88.5%, 90.2%, and 86.5%, respectively. The transmittance is obviously increased with the thermal annealing, especially for films annealed at temperatures of 300°C and 400°C.

The absorption coefficient ‘α’ was calculated using the following expression [13]:

$$\alpha = \frac{1}{t} \ln (1/T) \quad \dots\dots\dots(6)$$

where ‘T’ is transmittance, ‘t’ is the films thickness.

The direct optical band gap ‘E_g’ was determined by using equation:

$$\alpha h\nu = \beta_o (h\nu - E_g)^{\frac{1}{2}} \quad \dots\dots\dots (7)$$

Where ‘β_o’ is a constant, by plotting of (αhν)² versus hν as in Fig(4) and finding the intercept of curve with hν axis, optical band gap of thin films was determined. The estimated band gap energy values are listed in Table 4. These E_g are close to the values achieved by Camacho et al [3]. Some researchers have reported that orthorhombic SnO₂ phase has a wider band gap than that of the tetragonal phase. Kong et al. reported a value of 3.79 eV for the band gap of laser ablated orthorhombic SnO₂ [14]. Chen reported 4.02 eV for orthorhombic SnO₂ thin films obtained by laser ablation [15]. The band gap for tetragonal SnO₂ in bulk is 3.6 eV at 300 K[116].

One of the ways one can study the quality of a semiconductor thin films, is to investigate the Urbach energy and its variations, so the Urbach energy of the samples was determined from the exponential (absorption) edge region by using the following relation [11]:

$$\alpha = \alpha_0 e^{\frac{h\nu}{E_u}} \quad \dots\dots\dots (8)$$

where ‘α_o’ is a constant and ‘Eu’ is the Urbach energy, which characterizes the slope of the exponential edge. To obtain the value of E_u, the graph of ln(α) against hν is plotted (for hν < E_g), which is linear as shown in Fig(5) and the Urbach energy calculated from the inverse slope and listed in Table 4. Because the Urbach energy indicates the structural disorder of a semiconductor, so lower Urbach energy indicates the lower defects[17].

In order to use thin films in optical applications require accurate knowledge of the optical constants such as extinction coefficient, ‘k’ refractive index ‘n’ and dielectric constants (real ‘ε_r’ and imaginary part ‘ε_i’) over a wide wavelength. These constants can be evaluated using the relationships [11,17,18]:

$$k = \frac{\alpha\lambda}{4\pi} \quad \dots\dots\dots(9)$$

$$n = \left[\left(\frac{1+R}{1-R} \right)^2 - (k^2 + 1) \right]^{\frac{1}{2}} + \frac{1+R}{1-R} \quad \dots\dots\dots(10)$$

$$\epsilon_r = n^2 - k^2 \quad \dots\dots\dots(11)$$

$$\epsilon_i = 2nk \quad \dots\dots\dots(12)$$

The calculated values of extinction coefficient, refractive index real and imaginary part of dielectric constants were plotted as a function of the wavelength, as shown in fig(6)- Fig (9) respectively. It is seen that both, index real and imaginary part of dielectric constants decrease with increasing wavelength, the both parts follow the same pattern and the values of real part are higher than those of the imaginary parts, this due to that the optical constants are related to the density of states within the energy gap of the films.

The single-oscillator parameters were calculated and analyzed using the Wemple and DiDomenico single oscillator model. This model describes the dielectric response for transitions below the optical gap. This plays an important role in determining the behavior of the refractive index. The dispersion data of the refractive index can be described by a single-oscillator model [19].

$$n^2 - 1 = \frac{E_d E_o}{E_o^2 - (h\nu)^2} \dots\dots\dots(13)$$

Where ‘E_o’ is the average electronic energy gap for transition (average excitation energy) known as the oscillator energy, and ‘E_d’ is the dispersion energy (average strength of interband optical transition) called the oscillator strength. By plotting (n²-1)⁻¹ vs. (hν)² as in Fig (10) and fitting a straight line, the values of the parameters E_o and E_d were calculated from (E_o/E_d) represents the intercept on the vertical axis and (E_o E_d)⁻¹ is the slope of the plot and listed in table (4). We found that E_o value of the films is related to the direct band gap by E_o ≈ 1.2 Eg -1.4Eg, this is good agreement with the result of other worker[19,20].

Table 4 The estimated values of energy gap, Urbach energy and the oscillator parameters of SnO₂ thin films.

Samples	E _g eV	E _u eV	E _o eV	E _d eV
As- deposited at 200°C	3.68	1.385	5.21	14.02
Annealed at 300°C	3.72	0.950	4.62	5.26
Annealed at 400°C	3.71	1.056	4.45	6.78
Annealed at 500°C	3.70	1.278	4.83	8.75

III. Conclusions

The effects of annealing on the structural and the optical properties of SnO₂ thin films prepared by DC magnetron sputtering system were investigated. The grain size of the crystallites was found to be in the range of 14.4 nm - 26.3 nm. The optical transmission spectra in the transparent region were improved and the absorption edge shifted toward a shorter wavelength side by thermal annealing. From structural and optical measurements, it was observed that 300°C annealing temperature was mostly suitable for high quality SnO₂ films on glass substrate by DC magnetron sputtering system for opto-electronic devices fabrication.

References

- [1]. Wagner F., Transparent electronics, Science, 300 (2003) 1245.
- [2]. Presley R.E., Munsee C.L., Park C.-H., Hong D.J., Wager F. & Keszler D.A., J. Phys., D 37 (2004) 281.
- [3]. Camacho L. M. A., Galeana C. J. R., Esparza G. A., Sánchez C., Julien C. M., Superficies y Vacío, 26(3) septiembre de (2013)95.
- [4]. Prathyusha T., Seshendra Ch. R., Sreedhara P. R., Sivasankar A. R., International J. of Chem.Tech. Research, 6(6) (2014) 3349.
- [5]. Jiang J. C., Lian K. and Meletis E. I., Thin Solid Films, 411(2002) 203.
- [6]. Ramanathan G., John R.X. and Murali K.R., Elixir Thin Film Tech., 50 (2012) 10588.
- [7]. Wan C. F., McGrath R. D., Keenan W. F. and Frank S. N., J. Electrochem. Soc., 136(1989)1459.
- [8]. Mc Carthy, Welton G., J. Powder Diffraction, 4(1989) 156.
- [9]. Coskun C., Guney H., Gur E. and Tuzemen S., Turk. J. Phys., 33 (2009) 49.
- [10]. Cullity B.D., Elements of X-ray Diffraction, A. W. Pub. Comp. Inc, (1978) 99.
- [11]. Ilican S., Caglar X., Caglar M., Demirci B., J. of Optoelectronics and adv. mater., 10 (2008)2592.
- [12]. Lupan O., Pauporte T., Chow L., Viana B., Pelle´ F., Ono L.K., Roldan B.C., Heinrich H., Appl. Surf. Sci. 256 (2010) 1895
- [13]. Roy S. S. and Podder G. J., J. Optoelectronics and Adv. Mater., 12 (2010)1479.
- [14]. Kong L., Ma J., Zhu Z., Luan C., Yu X., Yu Q., Mater. Lett., 64, (2010)1350.
- [15]. Chen Z. W., Wu C. M. L., Shek C. H., Lai J. K. L., Jiao Z., Wu M. H., Critical Reviews in Solid State and Materials Sciences, 33 (2008) 197.
- [16]. Fang L. M., X. T. Zu, Z. J. Li, S. Zhu, C. M. Liu, L. M. Wang, and F. Gao, J. Mater. Sci: Mater. Electron., 19 (2008) 868.
- [17]. Peko J.I., Optical processes in semiconductors, Prentice-Hall, New York(1971).
- [18]. Hazaa S.K., Berkala Fisika Indonesia, 5 (1) Januari (2013)1.
- [19]. Wemple S.H., DiDomenico M., Phys. Rev., B 3 (1971) 1338.
- [20]. Ilican S., Caglar Y., Caglar M., Physica Macedonica, 56(2006)43.

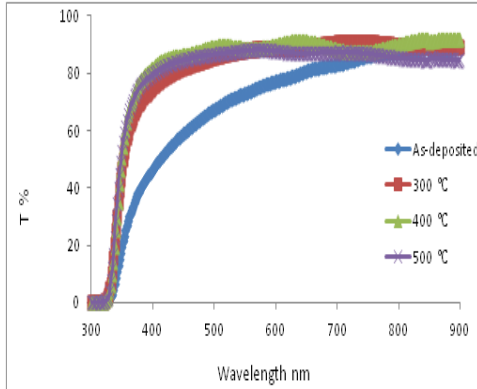


Fig.3. Transmittance spectra for the SnO₂ thin films

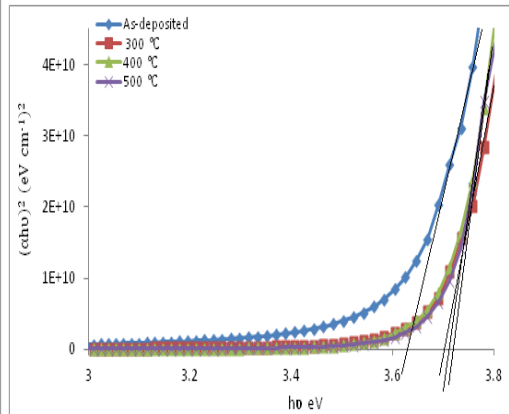


Fig.4. Plots of $(\alpha h\nu)^2$ with $h\nu$ of SnO₂ thin films

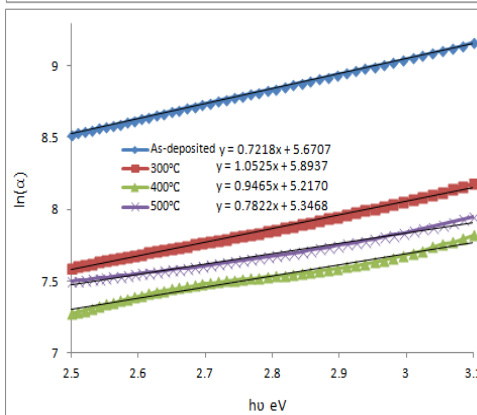


Fig.5. Variation of $\ln(\alpha)$ with photon energy

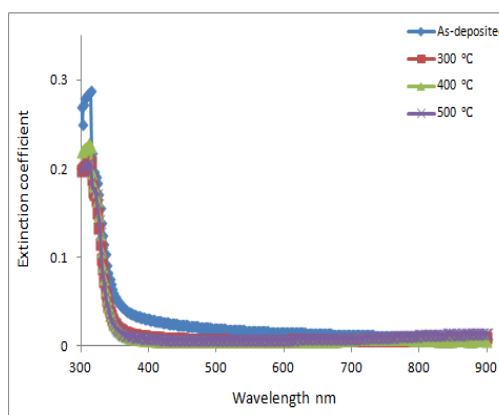


Fig.6. Variation of extinction coefficient with wavelength

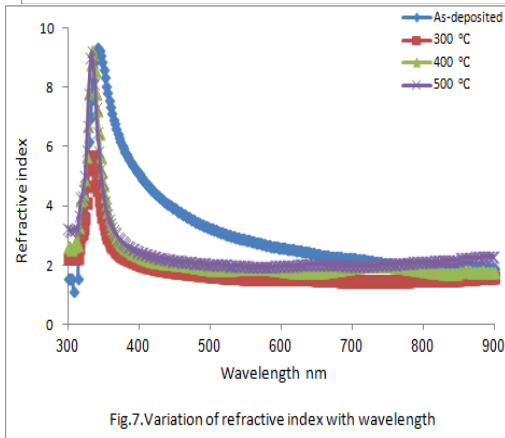


Fig.7. Variation of refractive index with wavelength

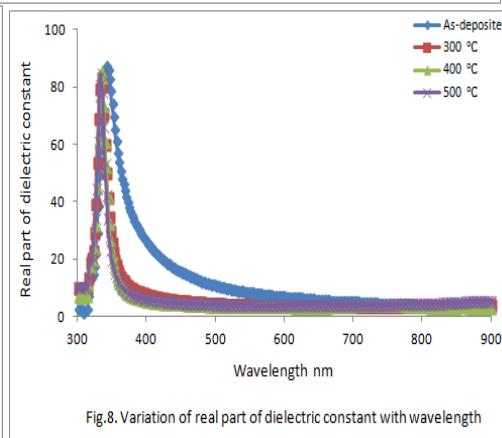


Fig.8. Variation of real part of dielectric constant with wavelength

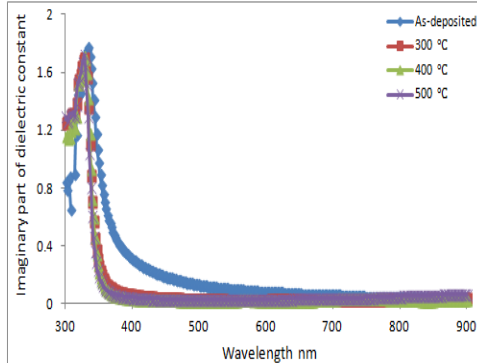


Fig.9. Variation of imaginary part of dielectric constant with wavelength

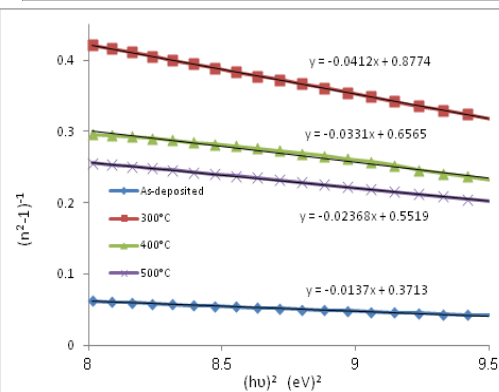


Fig.10. Plots of $(n^2-1)^{-1}$ against $(h\nu)^2$ for SnO₂ films.